

Surfactant-Mediated Growth Revisited

H. L. Meyerheim,¹ D. Sander,¹ R. Popescu,^{1,*} W. Pan,^{1,†} I. Popa,² and J. Kirschner¹

¹Max-Planck-Institut für Mikrostrukturphysik, Weinberg 2, D-06120 Halle, Germany

²ESRF, BP 220, F-38043 Grenoble, France

(Received 23 March 2007; published 11 September 2007)

The x-ray structure analysis of the oxygen-surfactant-mediated growth of Ni on Cu(001) identifies up to 0.15 monolayers of oxygen in subsurface octahedral sites. This questions the validity of the general view that surfactant oxygen floats on top of the growing Ni film. Rather, the surfactant action is ascribed to an oxygen-enriched zone extending over the two topmost layers. Surface stress measurements support this finding. Our results have important implications for the microscopic understanding of surfactant-mediated growth and the change of the magnetic anisotropy of the Ni films.

DOI: [10.1103/PhysRevLett.99.116101](https://doi.org/10.1103/PhysRevLett.99.116101)

PACS numbers: 68.35.Ct, 61.10.-i, 75.70.Ak

A well-established procedure to obtain atomically flat films in heteroepitaxial and homoepitaxial growth is the application of so-called surfactants. These surfactants are deposited onto the substrate surface prior to or during film growth and lead to an atomically flat morphology of the deposited film, as discussed in numerous studies [1–7].

The surfactant action has been ascribed in a thermodynamical description to the surfactant-induced lowering of the surface free energy [1]. Recent experimental and theoretical works have identified surfactant-induced modifications of the atomic diffusion processes on surfaces and at steps as essential aspects for the improved 2D growth [3,4,8,9].

This picture of the surfactant action leads to the widely accepted assumption that the surfactant floats on the outer surface of the growing film. In view of the involved bond-breaking and diffusion steps of the surfactant during film growth, this is a most remarkable hypothesis, and it awaits experimental justification.

Whereas the surfactant action leading to an improved 2D growth has been explored for many systems, studies of the atomic structure at the substrate-film and the film-vacuum interface of a surfactant growth system are scarce.

It is the goal of this study to clarify the exact atomic position of a surfactant after termination of surfactant-mediated growth. To this end we have investigated a prototype system, namely, the oxygen-mediated growth of Ni on Cu(001). The use of oxygen as a surfactant for the subsequent Ni growth starts with the preoxidized Cu(001) surface, which exhibits the missing-row (MR) ($\sqrt{2} \times 2\sqrt{2}$) $R45^\circ$ reconstruction. Subsequent Ni adsorption leads to an improved layer-by-layer growth. It has been proposed that here oxygen floats on top of the Ni surface, where it forms a $c(2 \times 2)$ -O structure [10,11].

In addition to its importance as a surfactant, oxygen has been identified to reduce the surface magnetic anisotropy energy (K_{S1}) of the Ni film. It induces a reduction of the film thickness from 11 monolayer (ML) (clean Ni film) to 5 ML (oxygen covered) at which the “unusual” spin-reorientation transition (SRT) from in plane to out of plane

takes place. Recent work has identified a delicate interplay between subtle structural details, adsorbate coverage, and the magnetic anisotropy of this system [5,11–15].

Our surface x-ray diffraction (SXRD) and stress measurements clearly indicate that the previous structural model is too simple. We find compelling evidence for oxygen in subsurface octahedral interstitial sites. Thus, the surfactant action of oxygen should rather be ascribed to an oxygen-enriched zone near the surface of the growing film. Former work has lacked the high layer resolved sensitivity and accuracy of our SXRD structure analysis. Thus, although the former conclusions were in agreement with previously published data, they miss decisive aspects of the structural and chemical details near the top surface, which are presented here.

We find substantial structural relaxation and chemical inhomogeneity in the two topmost surface layers. This calls for a reexamination of the mechanisms of surfactant-mediated growth and for the previously found modified magnetic anisotropy of surfactant-grown Ni monolayers [5].

Experiments were performed in two separate UHV systems optimized for SXRD and *in situ* stress measurements, respectively. The SXRD experiments were carried out at the beam line ID03 of the European Synchrotron Radiation Facility in Grenoble, France. SXRD is well suited to precisely analyze the bonding geometry at surfaces and interfaces [16], including even submonolayer quantities of oxygen [17].

The same crystal preparation by ion bombardment (Ar^+ , 1 keV) and subsequent annealing at 720 K was performed for stress and SXRD experiments prior to oxygen adsorption and Ni deposition. The ($\sqrt{2} \times 2\sqrt{2}$) $R45^\circ$ reconstruction was formed by exposing Cu(001) at 500 K to a partial pressure of oxygen of 10^{-6} mbar and was monitored by measuring a characteristic superlattice reflection. Similarly, the deposition rate of the subsequently deposited Ni film was calibrated by monitoring the intensity oscillations of the (1 0 0.1) crystal truncation rod (CTR) reflection intensity close to the (100) antiphase condition (indexing

of the reflections is based on the primitive setting of the surface unit cell).

Stress measurements were performed by the crystal curvature technique, where the stress-induced change of curvature of a 0.1 mm thin Cu(001) crystal is monitored by an optical deflection technique [18]. Thus, the adsorbate-induced change of surface stress τ_S and the stress τ during deposition of a film of thickness t_F are determined with high accuracy (± 0.05 N/m). Oxygen-induced surface stress changes during oxygen exposure at 500 K and low-energy electron-diffraction (LEED) pattern were recorded to identify the formation of the missing-row reconstruction [18]. Medium-energy electron-diffraction intensity oscillations were used to calibrate the Ni growth rate in the stress measurement.

The stress measurements of Fig. 1 provide compelling evidence that the previously supported view of oxygen floating on top of the Ni film after completion of oxygen-mediated surfactant growth is not appropriate. The solid (blue) curve indicates that the deposition of 8 ML Ni on Cu(001) (1 ML \cong 0.17 nm) induces a tensile stress of 5.13 ± 0.05 N/m. This stress change is ascribed to the lattice misfit induced film stress [19].

The stress change during Ni deposition onto the O-induced MR reconstruction of Cu(001) is shown by filled (red) circles. This scenario corresponds to the previously described O-mediated surfactant growth of Ni on Cu [5]. Here, the overall stress change after deposition of 8 ML is 4.64 ± 0.05 N/m. After deposition, LEED and SXRD identify a $c(2 \times 2)$ -O surface structure. To compare the overall stress change between both growth modes, we need to consider the O-induced surface stress change of the Ni film.

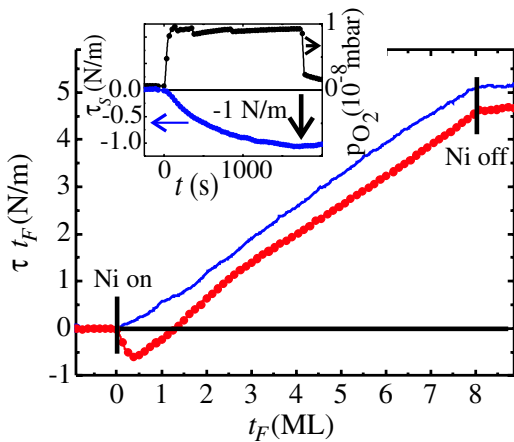


FIG. 1 (color online). Stress change during deposition of 8 ML Ni on Cu(001) (solid line) and on the missing-row reconstructed ($\sqrt{2} \times \sqrt{2}$) $R45^\circ$ Cu(001) (filled circles). Inset: Surface stress change during O_2 exposure of the 8 ML Ni/Cu(001) system, leading to a $c(2 \times 2)$ -O structure. All measurements were performed at 300 K.

Thus, we also measured the surface stress change due to the formation of a $c(2 \times 2)$ -O surface structure on top of the 8 ML Ni film. The O-surface structure is prepared by exposing the Ni film to a partial pressure of oxygen of 1×10^{-8} mbar at 300 K for 1730 s, as shown in the inset of Fig. 1. We measure an O-induced compressive surface stress change of -1.0 ± 0.05 N/m, as shown in the lower curve of the inset of Fig. 1. We conclude that the overall stress change starting from clean Cu(001) and ending with a $c(2 \times 2)$ -O/8 ML Ni/Cu(001) system amounts to 4.13 ± 0.07 N/m. This differs significantly from the value of 4.64 N/m measured for the O-mediated surfactant growth.

We find a 0.51 N/m larger stress change for the O-surfactant-mediated growth as compared to Ni film growth, followed by O adsorption. We take this as a direct hint that the resulting O-Ni-Cu systems are not identical, and this contrasts with the picture presented in previous work on the surfactant action of oxygen. We do not observe the full stress relaxation for the O-surfactant growth as compared to the $c(2 \times 2)$ -O structure on top of Ni(001) suggesting that not all of the oxygen floats on top of the Ni film, which was prepared under O-surfactant growth conditions. The following SXRD analysis identifies up to 15% of a ML oxygen residing in subsurface sites, which offers a conclusive explanation why a smaller O-induced stress relaxation is observed.

Four different and independent samples with a Ni film thickness of 1.25, 2.25, 3.00, and 5.00 ML deposited on the missing-row reconstructed Cu(001) surface were analyzed. For each preparation in total about 330 reflections along four symmetry independent CTRs and two superlattice rods (SLRs) characteristic for the $c(2 \times 2)$ superstructure were collected reducing to about 230 by symmetry equivalence. The structure factor amplitudes $|F|$ were derived from the integrated intensities by correcting the data for geometric factors [20].

Solid symbols in Figs. 2(a)–2(c) represent the $|F|$'s for the 1.25 ML sample along the (10ℓ) and (11ℓ) CTR [2(a) and 2(b)] as well as along the $(1/2 \ 1/2 \ \ell)$ and the $(3/2 \ 1/2 \ \ell)$ SLRs [2(c)], respectively. In the case of the CTRs we focus on the surface sensitive, low intensity regime between the bulk Bragg reflections, characterized by the condition $h + k + \ell = 2n$ with n integer.

The solid (black) lines of Fig. 2 represents the best fit to the experimental data. The fit quality is expressed by the unweighted residuum (R_u) and by the goodness of fit (GOF) parameter [21]. The latter considers experimental uncertainties and the relation between the number of data points and fitting parameters. The high symmetry of the structure justifies that for each atomic position only the z parameter needs to be varied leading to 10–20 free parameters ensuring a significant overdetermination of the refinement problem. The analysis further benefits from low correlations ($|C| < 0.7$) between the parameters. For R_u

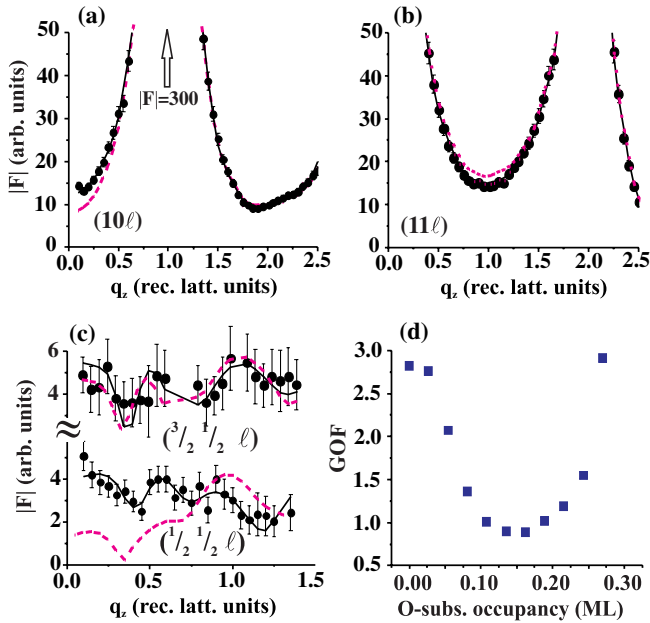


FIG. 2 (color online). (a)–(c) Measured (symbols) and calculated (lines) structure factor amplitudes for 1.25 ML Ni/O/Cu(001)- $c(2 \times 2)$. Black (solid) and red (dashed) lines represent fits corresponding to the structure models with subsurface oxygen and surface oxygen only, respectively. (d) GOF parameter versus oxygen subsurface occupancy.

and GOF, values as low as 0.047 and 0.90, respectively, were achieved, indicating the excellent fit quality.

We derive a complex surface structure, where layer buckling and different oxygen positions are found. Up to about 1/3 of the total amount of oxygen resides in subsurface sites within the second layer while the remaining fraction is located in surface hollow sites. The overall O content is found by SXRD to be 0.5 ML, indicating that all oxygen is bound in an ordered structure.

The structure model for 1.25 ML Ni serves as a representative example, which is shown in Fig. 3. Surface oxygen atoms reside in hollow sites at $h = 0.3\text{--}0.4 \text{ \AA}$ ($\pm 0.05\text{--}0.10 \text{ \AA}$) above the top Ni layer, in reasonable agreement with theoretical predictions (0.51 \AA) [11], and in very good agreement with surface extended x-ray absorption fine structure experiments (0.41 \AA). This corresponds to a Ni-O bond length of 1.85 \AA [7]. We also find

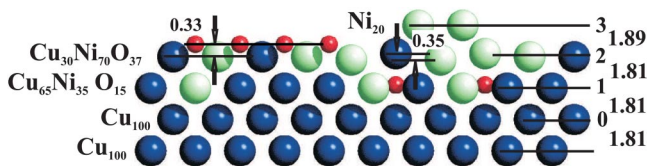


FIG. 3 (color online). Structure model for 1.25 ML Ni/O/Cu(001). Blue (dark), green (gray), and small (red) spheres represent Cu, Ni, and O atoms, respectively. Layer stoichiometry is given on the left. Distances are given in angstroms. Layers are numbered from 0 to 3.

rumpling within the topmost layer, where the atoms directly above the subsurface oxygen atoms are shifted upwards by 0.21 \AA , while those with no oxygen beneath are shifted downwards by 0.14 \AA leading to a total rumpling of 0.35 \AA , as indicated in Fig. 3. Rumpling is attributed to the accommodation of oxygen interstitial atoms. Without rumpling, the interstitial O-Ni bond length would be as small as 1.81 \AA . With rumpling, the local structure around the interstitial oxygen is still under anisotropic strain due to the short Ni-O distance of 1.85 \AA (out of plane) and 1.81 \AA (in plane), as compared to the bulk Ni-O bond length of 2.08 \AA . We conclude that interstitial oxygen is energetically favorable only in the subsurface site, where stress relief is possible by top-layer rumpling. We propose that this structural aspect originally discussed by Tersoff [22] in the context of surface alloy formation in lattice mismatched systems limits the distribution of oxygen to the hollow site on top and to the interstitial sites in the subsurface layer and provides an explanation for the segregation behavior of the oxygen-surfactant layer.

Subsurface oxygen is necessary to obtain a high fit quality. To illustrate this point, we show the dashed (red) lines in Fig. 2, where we wrongly consider exclusively surface oxygen. This leads to a bad fit of the data points characterized by almost threefold increased quality factors ($R_u = 0.107$ and $\text{GOF} = 2.82$) as compared to the proper model (black solid lines). The dependence of the GOF on the oxygen subsurface occupancy is shown in Fig. 2(d). The smallest GOF value is obtained for an oxygen occupancy in the subsurface site of $\theta \approx 0.15 \text{ ML}$. Any deviation from the optimum value leads to a worse fit quality, such as, e.g., $\text{GOF} = 2.82$ in the case of no oxygen in interstitial sites at $\theta = 0 \text{ ML}$.

Note that subsurface oxygen has been identified before in studies on the catalytic activity of metal substrates [23,24]. Our results show that even moderate exposure under UHV conditions at 300 K leads to subsurface oxygen.

The evolution of the interface structure with Ni coverage is summarized in Fig. 4. For achieving high quality fits all details of the near surface structure including surface roughness (incomplete layers) and adsorption of oxygen thereon are taken into account. Subsurface oxygen is always present in concentrations up to nearly 20% of a ML. At larger Ni coverage, the subsurface oxygen concentration slightly decreases, but stays well above the detection limit of about 0.05 ML. In agreement with previous studies [11], oxygen atoms remain in the surface region with increasing Ni coverage. This result suggests that surface and interstitial oxygen float at the top of the growing film. Thus, the former picture of oxygen floating on top during Ni growth should be replaced with an oxygen-enriched zone, extending over the two topmost layers of the Ni film.

The SXRD analysis offers an explanation for the smaller stress relaxation for oxygen-mediated surfactant growth

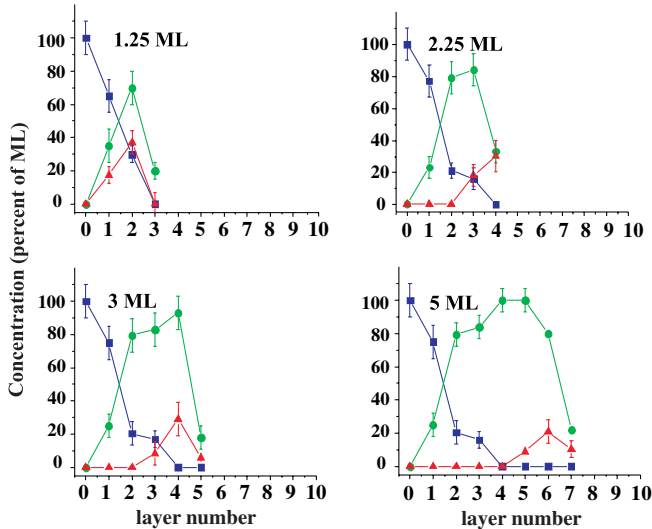


FIG. 4 (color online). Layer resolved concentrations in percent of a ML for Cu (blue squares), Ni (green circles), and oxygen (red triangles). Layer 0 corresponds to the topmost pure Cu layer, as shown in Fig. 3.

as compared to oxygen adsorption on a Ni film. Previous work on the oxygen-induced change of surface stress of metallic systems has shown a monotonously decreasing surface stress with oxygen surface coverage [18]. Thus, the smaller surface coverage of oxygen for the surfactant growth (0.3–0.4 ML) as compared to oxygen adsorption on Ni (0.5 ML) is expected to induce a smaller surface stress relaxation, in agreement with our stress measurements.

Oxygen in subsurface interstitial sites reveals a driving force for surface rumpling and local strain variations within the surface layer. Surface strain has an important impact on surface diffusion [25]. We propose that the surfactant-induced variation of the strain within the surface region is another factor, which leads to the surfactant action of an adsorbate.

Our results of oxygen in subsurface octahedral interstitial position has also considerable impact on the discussion of the modified magnetic anisotropy of surfactant-grown Ni films. Previous studies have considered a sizable reduction of the magnetic surface anisotropy (K_{S_1}) from -107 to $-17 \mu\text{eV}/\text{atom}$, which drives the oxygen-induced shift of the SRT from in plane to out of plane of Ni films [10]. Calculations reproduce the oxygen-induced reduction of the magnitude of K_{S_1} qualitatively; quantitatively a small positive value for K_{S_1} of the O/Ni interface is found [5], in contradiction with experimental results. Although most structural details of the calculations [5], such as the expanded top-layer spacing (1.84 Å) and the presence of some rumpling in the subsurface layer (0.03 Å), are in reasonable agreement with our experimental results, the calculations neglect subsurface oxygen, and its effect on

K_{S_1} is not included. In view of the intimate relation between magnetic properties and structural details of this system [15], future calculations need to include oxygen in subsurface octahedral interstitial sites. This may resolve the discrepancy between experiment and calculation regarding K_{S_1} in the description of the oxygen-induced SRT.

In summary, our SXR study of the oxygen-surfactant-mediated growth of Ni on Cu(001) has revealed that a significant fraction ($\approx 1/3$ of the deposited oxygen) resides in subsurface octahedrally coordinated interstitial sites involving lattice distortions and compositional inhomogeneity. This suggests a revision of the traditional view of surfactant action by considering a surfactant-enriched zone rather than a surfactant adsorbed on top of the growing film. The corresponding rumpling of the surface layers needs to be considered for the understanding of the surfactant action and its role for surface stress relaxation and magnetic anisotropy.

H. L. M., D. S., R. P., and W. P. thank the ESRF staff for their help and hospitality during their stay in Grenoble.

*Also at: Labor für Elektronenmikroskopie, Universität Karlsruhe, D-76128 Karlsruhe, Germany.

†Also at: Department of Physics, National Chung Cheng University, Chia-Yi 62102 Taiwan.

- [1] W. F. Egelhoff, Jr. *et al.*, *J. Vac. Sci. Technol. A* **7**, 2167 (1989).
- [2] H. A. van der Vegt *et al.*, *Phys. Rev. Lett.* **68**, 3335 (1992).
- [3] St. Esch *et al.*, *Phys. Rev. Lett.* **72**, 518 (1994).
- [4] H. A. van der Vegt *et al.*, *Phys. Rev. B* **57**, 4127 (1998).
- [5] J. Hong *et al.*, *Phys. Rev. Lett.* **92**, 147202 (2004).
- [6] M. Nyvlt *et al.*, *Phys. Rev. Lett.* **95**, 127201 (2005).
- [7] C. Sorg *et al.*, *Phys. Rev. B* **73**, 064409 (2006).
- [8] M. Jiang *et al.*, *J. Phys. Condens. Matter* **10**, 8653 (1998).
- [9] J. Ferrón *et al.*, *Surf. Sci.* **459**, 135 (2000).
- [10] J. Lindner *et al.*, *Surf. Sci.* **523**, L65 (2003).
- [11] R. Nünthel *et al.*, *Surf. Sci.* **531**, 53 (2003).
- [12] S. Hope *et al.*, *Phys. Rev. Lett.* **80**, 1750 (1998).
- [13] R. Vollmer *et al.*, *Phys. Rev. B* **60**, 6277 (1999).
- [14] S. van Dijken *et al.*, *J. Magn. Magn. Mater.* **210**, 316 (2000).
- [15] D. Sander *et al.*, *Phys. Rev. Lett.* **93**, 247203 (2004).
- [16] I. K. Robinson *et al.*, *Rep. Prog. Phys.* **55**, 599 (1992).
- [17] C. Tusche *et al.*, *Phys. Rev. Lett.* **95**, 176101 (2005).
- [18] M. J. Harrison *et al.*, *Phys. Rev. B* **74**, 165402 (2006).
- [19] Th. Gutjahr-Löser, Ph.D. thesis, Universität Halle, Germany, 1999.
- [20] E. Vlieg, *J. Appl. Crystallogr.* **30**, 532 (1997).
- [21] R_u is defined as $R_u = \frac{\sum ||F_{\text{obs}}| - |F_{\text{calc}}||}{\sum |F_{\text{obs}}|}$ with F_{obs} and F_{calc} as observed and calculated structure factors, respectively. For GOF see Ref. [16].
- [22] J. Tersoff, *Phys. Rev. Lett.* **74**, 434 (1995).
- [23] B. Pettinger *et al.*, *Phys. Rev. Lett.* **72**, 1561 (1994).
- [24] L. Savio *et al.*, *Appl. Phys. A* **87**, 399 (2007).
- [25] D. V. Tsivilin *et al.*, *Phys. Rev. B* **68**, 205411 (2003).